Journal of Chromatography B, 885–886 (2012) 73–82

Contents lists available at SciVerse ScienceDirect

Journal of Chromatography B

journal homepage: www.elsevier.com/locate/chromb

Identification of metabolites of Si-Ni-San, a traditional Chinese medicine formula, in rat plasma and urine using liquid chromatography/diode array detection/triple–quadrupole spectrometry

Zhixiang Yan[a], Ying Chen[a], Tianxue Li[a], Jie Zhang[b], Xinghao Yang[a,*]

[a] Laboratory of Pharmaceutics, Jiangsu Key Laboratory for Molecular and Medical Biotechnology, College of Life Sciences, Nanjing Normal University, Nanjing 210046, People's Republic of China
[b] Analysis and Test Center, Nanjing Normal University, Nanjing 210097, People's Republic of China

ARTICLE INFO

Article history:
Received 6 August 2011
Accepted 18 December 2011
Available online 26 December 2011

Keywords:
Si-Ni-San
Metabolite
Liquid chromatography coupled with diode array detection
Triple–quadrupole spectrometry
n-Octanol/water partition coefficient

ABSTRACT

Si-Ni-San (SNS) is a widely used traditional Chinese medicine formula (TCMF) in treating various diseases. However, the *in vivo* integrated metabolism of its multiple components remains unknown. In this paper, a liquid chromatography coupled with diode array detection and triple–quadrupole spectrometry (LC-DAD–MS/MS) method was developed for detection and identification of SNS metabolites in rat plasma and urine at a normal clinical dosage. Accurate structural elucidation was performed using MS/MS, UV data and n-octanol/water partition coefficient. Based on the proposed strategy, 36 absorbed compounds and 29 metabolites in plasma and 33 metabolites in urine were detected by a highly sensitive MRM method. Our results indicated that phase II reactions (*e.g.*, methylation, glucuronidation and sulfation) were the main metabolic pathways of gallic acid and flavanones, while phase I reactions (*e.g.*, hydroxylation) were the major metabolic reaction for triterpenoid saponins. The metabolite profile analysis of SNS provided a comprehensive understanding of the *in vivo* metabolic fates of constituents in SNS. Moreover, the results in this work demonstrated the present strategy based on the combination of chromatographic, spectrophotometric, mass-spectrometric, and software prediction to detect and identify metabolites was effective and reliable. And such a strategy may also be extended to investigate the metabolism of other TCMF.

1. Introduction

Si-Ni-San (SNS), a famous traditional Chinese medicine formula (TCMF), derived from *Treatise on febrile diseases*, a medical classic by Zhang Zhongjing published in 220 AD. The prescription comprises an equal ratio of four drugs: Radix *Bupleuri*, Radix *Glycyrrhizae Preparata*, Fructus *Aurantii Immaturus*, and Radix *Paeoniae Alba*. SNS has been widely used to treat hepatitis, gastritis, neuralgia, appendagitis, *etc.*, in clinics [1–3]. The recent study on SNS showed that it possessed strong effect in treating immunological liver injury and contact sensitivity [4,5].

In the past few years, several researches [6,7] have studied the role of saikosaponin, paeoniflorin, naringin, and glycyrrhizin in SNS. The results indicated that saikosaponin a and glycyrrhizin may be the major contributors in the alleviation effect of Si-Ni-San on contact sensitivity, and paeoniflorin and naringin may exhibit a co-operative effect. Furthermore, a selective deletion method was applied to validate paeoniflorin and glycyrrhizin as the active ingredients [8,9]. The contents of these four compounds in SNS have been determined in our previous research by RP-HPLC [10]. Another anion-exchange chromatography method was also used to quantify paeoniflorin and albiflorin in SNS [11]. However, unlike the synthetic drugs, TCM exerts the efficacy based on the synergic effects of their multi-components and multi-targets. The focus on a few bioactive components is insufficient for clarifying the detailed active principles and overall action mechanism of SNS. Therefore, we used a HPLC-DAD–MS/MS method to systematically study chemical constituents of SNS [12]. Their MS, UV data (Table S1) and chemical structures (Fig S1) are shown in the supplementary material. According to the chemical structures, the major compounds in SNS could be classified into three groups: monoterpene glucosides (include paeoniflorin, albiflorin, *etc.*), flavonoids (include naringin, hesperidin, *etc.*) and triterpenoid saponins (include glycyrrhizic acid, licorice saponin G2, *etc.*). Considering that *in vivo* metabolism study is closely related to the bioactivity of SNS, it was necessary to perform *in vivo* investigation of SNS to validate the conclusion from *in vitro* studies and to delineate the complete absorption, distribution, metabolism, and elimination (ADME) processes of SNS.

* Corresponding author. Tel.: +86 25 85891871; fax: +86 25 85891526.
E-mail addresses: yangxinh@126.com, godfnxk@163.com (X. Yang).

1570-0232/$ – see front matter © 2011 Elsevier B.V. All rights reserved.
doi:10.1016/j.jchromb.2011.12.017

The chemical profiling of SNS in plasma will reduce the number of chemicals involved for further investigations and help to reveal the potential active principles. However, the low concentrations of some components in the plasma would make them very hard to be detected. On the other hand, due to renal tubular reabsorption, the concentrations of many compounds and metabolites in urine are much higher than those in plasma. Thus, it would be easier to elucidate chemicals' ADME characteristics and the active principles of SNS by combining the information obtained from the two biological matrices [13].

Today, tandem mass spectrometry is used as a routine basis for structure elucidation of metabolites. Three types of mass analyzer are commonly used, *i.e.*, quadrupole (Q) [14], ion trap (IT) [15], and time-of-flight (TOF) [16].

More recently, hybrid instruments such as quadrupole (linear) ion trap [17] and Fourier transform ion-cyclotron resonance (FT-ICR) [18,19] mass analyzers are used. Hybrid instruments, however, are extremely expensive, which makes them unavailable or impractical for most laboratories. In this work we used a triple–quadrupole instrument for the characterization of SNS metabolite. Meanwhile, due to the complex chemical nature, metabolic study of TCMF is more challenging and time-consuming than western drugs. In order to systematically characterize the metabolites of TCMF, a well designed strategy is needed. Therefore, we propose a novel strategy to systematically characterize the *in vivo* metabolites of SNS and this strategy could then be applied to investigate the metabolites of other TCMF.

2. Materials and methods

2.1. Chemicals, reagents and materials

HPLC-grade acetonitrile was purchased from Merck (Darmstadt, Germany). Formic acid and methanol (analytical reagent) were purchased from Shanghai Chemical Reagent Factory (Shanghai, China). Purified water (Wahaha Group Ltd., Hangzhou, China) was used for HPLC analysis. Distilled water was used for the extract and for the preparation of samples. Other organic solvents and chemical reagents used were of analytical grade and were purchased from Nanjing Chemical Reagent Co. (Nanjing, China). The crude drugs of Radix *Bupleuri*, Fructus *Aurantii Immaturus*, Radix *Paeoniae Alba*, and Radix *Glycyrrhizae Preparata* were purchased from Nanjing Lu Jiang Pharmaceutical Co. Ltd. (Nanjing, China) and were identified by Prof. Zhunan Gong at the College of Life Science, Nanjing Normal University. All authenticated samples were stored in the authors' laboratory. Authentic standards of liquiritin and glycyrrhizic acid were purchased from Nanjing Zelang Biological Technology Co. Ltd. (Nanjing, China).

2.2. SNS sample preparation for administration

The mixture of raw materials of Radix *Bupleuri* (25 g), Fructus *Aurantii Immaturus* (25 g), Radix *Paeoniae Alba* (25 g), and Radix *Glycyrrhizae Preparata* (25 g) were crushed into small pieces and refluxed with 1 L of ethanol–water (70:30, v/v) solution for 1.5 h. The filtrates were collected and the residues were then refluxed twice in 0.8 L of ethanol–water (70:30, v/v) solution for 1 h. Two batches of filtrate were combined and centrifuged at 3000 rpm for 5 min. The supernatant was concentrated to approximate 200 mL and then stored at 4 °C until use.

2.3. Animals and drug administration

Twenty-five male Sprague-Dawley rats (200 ± 20 g) were obtained from the Animal Multiplication Center of Qinglong Mountain (SCXK 2008-0033). The rats were randomly divided into five groups with 5 rats each (A, liquiritin group; B, glycyrrhizic acid group; C, high dose SNS group; D, blank group; E, normal dose SNS group). Animals were bred in a breeding room with temperature of 23 ± 2 °C, relative humidity of 60 ± 5%, and 12 h dark–light cycle. They were given standard laboratory water and food *ad libitum* and were maintained in metabolic cages. The experiment animals were housed under the above conditions for 1-week acclimation. They were fasted overnight with free access to water before drug administration and the fasting was continued for 12 h thereafter. The pure standards of liquiritin and glycyrrhizic acid were suspended in 0.5% CMC-Na and orally administered to rats at 100 mg/kg. The SNS extract was orally administered to rats ($n = 3$) at a high dose of 30 mL/kg (equal to 15 g/kg) and a normal dose of 1 g/kg, and the blank group was orally administered with physiological saline in the same way. Blood (0.5 mL from the ophthalmic veins) were collected under anesthesia at 0.5, 1, 2, 4 and 6 h after the administration. Urine samples were collected over 12 h at regular time intervals. Blood samples were collected in heparinized tubes and then centrifuged for 10 min at 4000 × *g*, 4 °C, and the supernatants (*i.e.*, the plasma) were stored at −70 °C until additional extraction and analysis. All plasma and urine samples from one group of rats were combined into one sample to eliminate the individual and time-dependent metabolic variability. The animal facilities and protocols were approved by the Institutional Animal Care and Use Committee, Nanjing Normal University (Nanjing, China). All procedures were in accordance with the National Institute of Health's Guidelines regarding the principles of animal care (2004).

2.4. Rat plasma and urine sample preparation

For urine samples, Supelclean™ LC-18 SPE cartridges (Sigma–Aldrich, St. Louis, MO) were used for sample extraction. 0.5 mL of urine samples was loaded onto SPE cartridges pre-conditioned with 2 mL methanol, followed by 2 mL H_2O. Loaded cartridges were washed with 2 mL H_2O and eluted with 4 mL methanol and the elution was evaporated to dryness at room temperature by nitrogen. Each plasma sample (0.5 mL) was placed in a 1.5 mL polypropylene tube, and 1 mL methanol was added to precipitate protein. The precipitated protein was removed by centrifugation at 13,000 × *g* for 10 min. The supernatant was subject to SPE by the same procedure as the urine samples described above. For LC–MS analysis the residue was dissolved in 1 mL methanol and then filtered through a 0.22 μm nylon filter. An aliquot of 5 μL was injected into the column.

2.5. Liquid chromatography

HPLC analysis was performed using an Agilent 1290 HPLC system equipped with a binary pump (G4220A), auto plate-sampler (G4226A), column oven (G1316C) and diode array detector (G4212A). The chromatography was performed on a Krosmasil C18 (250 mm × 6 mm, 5 μm) protected with an Agilent Zorbax Extend-C18 guard column (4.6 mm × 12.5 mm, 5 μm). Sample injection volume was 5 μL with needle wash and thermostatted autosampler was kept at 4 °C. The column temperature was maintained at 40 °C. Flow rate of mobile phase, consists of acetonitrile (A) and water–0.1% formic acid (B) was 0.6 mL/min and it was entirely introduced into the DAD–MS detection system. Gradient programmer was performed in the following manner: 5–12% A at 0–10 min, 20–35% A at 15–30 min, 64–100% A at 45–55 min. At the end of the run, 100% of acetonitrile was allowed to flush the column for 10 min, and an additional 10 min of post run time were set to allow for equilibration of the column with the starting eluant. The DAD detection was recorded between 200 and 400 nm and the

chromatographic profiles were registered at 254 nm, bandwidth 4 nm, reference off.

2.6. Mass spectrometry

Mass spectra were recorded on an Agilent 6460 Triple Quadrupole mass spectrometer (Agilent Technologies, USA) with Agilent Jet Stream Technology. Data acquisition was made with the qualitative analysis software (MassHunter Workstation, Agilent, USA). High purity nitrogen (N2) was used both as the nebulizing gas and drying gas. Ultra-high purity helium (He) was used as the collision gas. Detailed MS parameters were as follows: drying gas temperature: 350 °C, Drying gas flow: 11 L/min, sheath gas temperature: 400 °C, Sheath gas flow: 12 L/min, nebulizer pressure: 35 psig, fragment voltage: 120 V. The collision energy for collision-induced dissociation (CID) was initially set at 5 V and then adjusted in steps of 5 V according to the fragments. Spectra were acquired in negative ion mode with the mass range set at m/z 100–1000. Determination of appropriate MRM transitions and the optimization of parameters for the predicted metabolites were conducted by mass optimizer software (included with the MS system software). MS1 Resolution set to Unit and MS2 Resolution set to Unit. As there are no commercially available standards for the predicted metabolite molecules, a plasma and urine sample with a high dose of SNS was repeatedly analyzed using the optimizer software to set the parameters for those metabolites.

2.7. Software to calculate n-octanol/water partition coefficient (log P)

Software chembiodraw ultra 11.0 (Cambridgesoft®; Cambridge, MA) based on theoretical calculations was used to predict n-octanol/water partition coefficient (log P). The prediction of log P is based on 222 atomic contributions calculated from 1868 molecules by least squares analysis. This method allows a calculation of log P with a standard deviation of 0.43 log P units and can handle molecules containing hydrogen, oxygen, nitrogen, sulfur, halogens and phosphorus atoms. If this method is applied to molecules with internal hydrogen bonds, the standard deviation is 0.83 log P units.

3. Results and discussion

3.1. Optimization of chromatographic condition

To obtain HPLC chromatograms with good separation and peak shape, we used a low mobile phase flow rate of 0.6 mL/min, rather than the normal 1.0 mL/min, for the 4.6-mm HPLC column. On the other hand, a low LC flow rate was compatible to our ESI spray tip, and yielded maximum ionization efficiency. Given that SNS contains mostly phenolic compounds, an acidic mobile phase could improve both HPLC separation and compound ionization. Thus, 0.1% (v/v) formic acid was used as additives to adjust the pH value of the mobile phase. In the performance of gradient optimization, gradient time, gradient shape and initial composition of the mobile phase were taken into consideration, and the optimized gradient elution was presented in Section 2.5. Three column temperatures, 20 °C, 30 °C, and 40 °C, were tested and 40 °C gave the best result. Also, different wavelengths were monitored and compared. When the wavelengths were below 200 nm or above 400 nm, most components had weak or even no responses, so the DAD detection was performed in the range of 200–400 nm at 2 nm/step. For MS analysis the negative ion mode of ESI was selected for its better sensitivity.

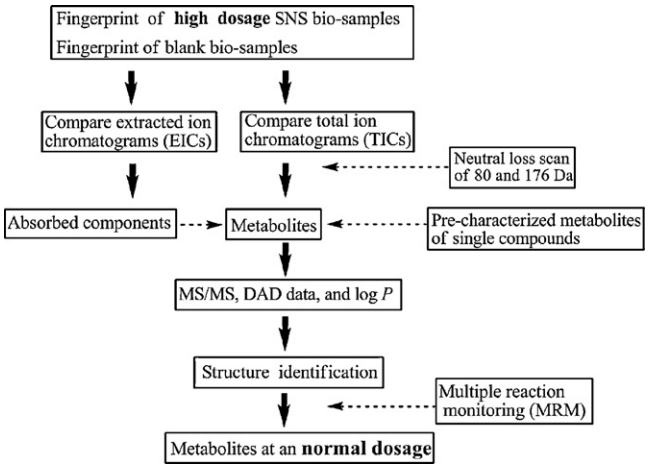

Fig. 1. Strategy for systematically characterization the *in vivo* metabolites of SNS at a normal dosage.

3.2. Strategy and approach for systematic analysis of metabolites

In the present work, we propose a novel strategy to systematically characterize the *in vivo* metabolites of SNS. An illustrative diagram was shown in Fig. 1. The strategy consisted of six steps: (1) characterize the metabolites of representative single compounds to reveal the metabolic pathways of each type of compounds; (2) screen absorbed components and metabolites by comparing extracted ion chromatograms (EICs) and total ion chromatograms (TICs) of high dosage SNS bio-samples with those from blank bio-samples (Fig. 2); (3) use a neutral loss scan of 80 and 176 Da to screen major glucuronide and sulfate conjugated metabolites (Fig. 3); (4) correlate MS and UV data of metabolites with those of parent compounds and pre-characterized metabolites derived from single compounds; (5) identify metabolites based on the MS/MS,UV data and n-octanol/water partition coefficient (log P); (6) profile metabolites in normal dosage bio-samples using multiple reaction monitoring (MRM) according to the pre-characterized metabolites in the high dosage bio-samples. The elaborations of strategy and approach were as follows.

3.2.1. Characterization of metabolites of single standards

TCMF contains multiple compounds with significant variety in structural types, physiochemical properties, and relative amounts. When they are administered by oral route, lots of compounds may get into circulation and then be converted into a mixture of metabolites of unknown origin. Meanwhile, chemicals in TCM usually present in the form of a series of analogues with the same skeleton but different functionalities and their metabolites may undergo similar fragmentation and produce some of the same aglycone ions. Understanding of the metabolic pathway of certain parent drugs will greatly facilitate metabolite identification of their analogues. Therefore we first studied the metabolic fate of single standards of two representative parent drugs including liquiritin and glycyrrhizic acid. As only one single compound was fed to rats, the metabolic profiles were easy to be elucidated. The result indicated that glucuronidation and sulfation predominated the metabolism of liquiritin, while hydrolysis was the major metabolic reaction for glycyrrhizic acid.

3.2.2. High dosage of administration

The low concentrations of drug metabolites and the high abundance of endogenous material in biological samples represent a considerable challenge for TCMF metabolites identification.

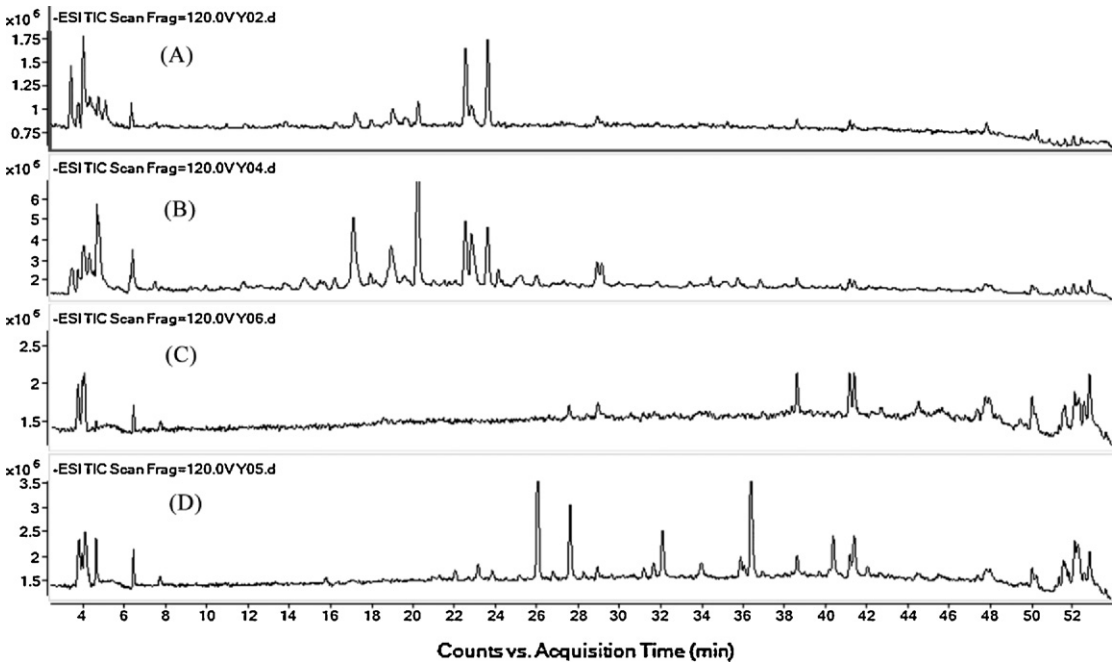

Fig. 2. Total ion chromatograms (TICs) in negative ion mode of (A) blank urine, (B) high dose of drug-containing urine, (C) blank plasma and (D) high dose of drug-containing plasma.

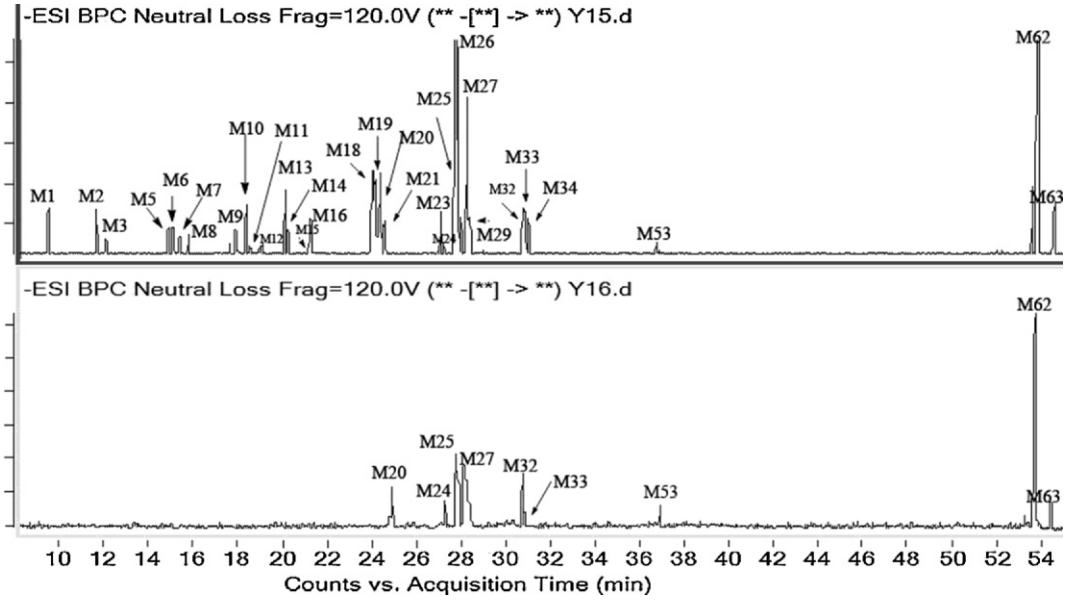

Fig. 3. Neutral loss scanning of 176 and 80 Da to screen glucuronide and sulfate conjugated metabolites in (A) high dose of drug-containing urine and (B) high dose of drug-containing plasma.

Comprehensive metabolite profiling of TCMF is usually hindered by their fairly low concentrations *in vivo* even using MS detector. Therefore, we gave a high dosage of SNS to rats to find more detectable metabolites.

3.2.3. *n*-Octanol/water partition coefficient (log *P*)

It was common that several metabolites were assigned as isomers in biological matrices. Elucidation and discrimination of the exact structure of these isomers, such as position of hydroxylation or conjugation, was challenging because little difference present in their MS spectra. MS will often provide only enough information to narrow down the choices to two or three possible structures. This holds true in particular if one of three hydroxyl groups undergoes metabolic conjugation. The n-octanol/water partition coefficient (log *P*) was also used in this study to locate the conjugation site. Log *P*, an important parameter in the process of designing new drugs, provides direct information on hydrophobicity that describes the tendency of distribution of a drug from aqueous phase into biological membranes [20]. Software chembiodraw ultra 11.0 was used to predict the relative retention time

of isomers and tentative assignment of their structure. In general, for compounds with log $P < 4$, the log P values are almost the same for both of experimental measurement and theoretical calculation and the large log P would have less retention time on the reverse phase-HPLC [21,22].

3.3. Characterization of absorbed components in high dosage bio-samples

From the point-of-view of pharmacokinetics, we know that only the compounds successfully absorbed into the blood may have the chance to show pharmacological bioactivities. The absorbed components were discovered by the extracted ion chromatograms (EICs). Peaks that were appeared both in dosed rat plasma and SNS at corresponding position but not in blank rat plasma were considered as the components absorbed into plasma. Once these peaks were determined to be the absorbed components, they were further confirmed by carefully comparing MS, MS/MS data, UV spectra, and retention times with that obtained from SNS. The structural information of parent compounds in SNS has been researched in our previous study (Table S1 and Fig S1). As a result, 44 components (Table 1) were found to be absorbed while the other minor components were not absorbed into rat plasma or their concentrations were to low to be detected. And we found most parent compounds including monoterpene glycosides, flavonoid glycosides and triterpenoid saponins could be absorbed.

3.4. Characterization of metabolites in high dosage bio-samples

The compounds absorbed into rat plasma were further metabolized by various drug metabolizing enzymes. These metabolic reactions can be divided into two cases called phase I and phase II reactions. Phase II metabolism is considered as the major detoxification pathway in the human body and glucuronidation and sulfation were the major metabolites of flavonoid glycosides [23–25]. Usually, glucuronidation and sulfation reactions make the drugs more hydrophilic, which can then be eliminated through bile and the kidney [26]. Common biotransformation pathways will result in predictable MS/MS fragmentation patterns, notably the neutral loss of 176 mass units for glucuronide conjugates and the loss of 80 mass units for sulfates. Thus, we first used a neutral loss scan of 80 and 176 Da to screen glucuronide and sulfate conjugated metabolites in urine (Fig. 3A) and plasma (Fig. 3B). As a result, 31 glucuronide and sulfate conjugates were detected which greatly facilitated the metabolite profiling of SNS. Comparing the total ion chromatograms (TICs) with that of blank bio-samples, another 34 metabolites were detected. Finally a total of 65 metabolites were detected from the drug-containing urine and plasma and 47 metabolites were characterized. All of the available information of metabolites was presented in Table 2. In this paper, we elaborated the identification of gallic acid-, flavanones- and glycyrrhizic acid-related metabolites as following because they were major metabolites of SNS. The structure elucidation of other metabolites was carried out similarly.

3.4.1. Identification of gallic acid-related metabolites

Nine compounds (M1–M8, M34) detected in rat urine were tentatively assigned as metabolites originating from gallic acid, among which M1–M3, M5–M8, and M34 were identified as glucuronide and sulfate conjugates (Fig. 3A). M1 gave a deprotonated molecule $[M-H]^-$ at m/z 301. Its MS/MS fragmentation was predominated by the elimination of glucuronidyl residue to give ion at m/z 125. The [glucuronic acid−H]-ion at m/z 175 could also be observed (Fig. 4A). According to the MS data and metabolic fate of gallic acid in rat [27], M1 was identified as pyrogallol-O-glucuronide. M2 and M3 both gave a $[M-H]^-$ ion at m/z 263 and exhibited a series of product ions at m/z 183, 168 and 124 (Fig. 4B), suggesting that they were isomeric sulfated metabolites with methyl-O-gallic acid aglycone. Previous urinary metabolism study of gallic acid in rats has confirmed the presence of 4-O-methylgallic acid-3-O-sulfate with authentic standard [28] According to the fact the large log P would have less retention time on the reverse phase-HPLC, M2 (11.70 min, log $P = -0.578$)

Table 1
Compounds absorbed in rat plasma after oral administration of a high dosage (H) and normal dosage (N) of SNS.

No.	t_R (min)	Identification	MRM transition	H	N	No.	t_R (min)	Identification	MRM transition	H	N
A1	15.79	Paeoniflorin sulfonate	543 > 121	+[a]	+	A23	39.36	Hesperetin	301 > 151	+	+
A2	17.21	Oxypaeoniflorin	495 > 137	+	+	A24	40.33	Glycyrrhizic acid	821 > 351	+	+
A3	21.21	Albiflorin	479 > 121	+	+	A25	40.69	Isoliquiritigenin	255 > 135	+	+
A4	22.08	Paeoniflorin	479 > 121	+	+	A26	41.76	Licorice saponin B2 isomer	807 > 351	+	+
A5	22.8	Liquritigenin apioside isomer	549 > 255	+	+	A27	41.89	Uralsaponin B	821 > 351	+	+
A6	23.43	Liquritigenin apioside	549 > 255	+	+	A28	42.34	Fomononetin	267 > 252	+	+
A7	24.22	Liquiritin [a]	417 > 255	+	+	A29	42.52	Licorice saponin H2 or K2	821 > 351	+	+
A8	25.39	Isonaringin	579 > 271	+	+	A30	42.78	Saikosaponin A	779 > 471	+	+
A9	25.74	Isoviolanthin	577 > 487	+	–	A31	42.91	Licorice saponin J2	823 > 351	+	+
A10	26.17	Naringin	579 > 271	+	+	A32	45.93	Licobenzofuran	353 > 297	+	+
A11	26.92	Hesperidin	609 > 301	+	+	A33	47.09	Licochalcone D	353 > 323	+	+
A12	28.01	Neohesperidin	609 > 301	+	+	A34	48.3	Licoisoflavone A	353 > 297	+	+
A13	28.46	Isoliquritigenin apioside	549 > 255	+	+	A35	48.67	Gancaonin L	353 > 285	+	+
A14	29.13	Licuraside	549 > 255	+	+	A36	50.07	Unidentified	407 > 381	+	+
A15	29.90	Isoliquiritin	417 > 255	+	+	A37	50.34	Unidentified	353 > 338	+	–[b]
A16	30.71	Neoisoliquiritin	417 > 255	+	+	A38	50.56	Glabrone	353 > 285	+	+
A17	33.75	Liquiritigenin	255 > 135	+	+	A39	51.23	Gancaonin M	351 > 323	+	–
A18	34.9	Licorice saponin A3	983 > 821	+	+	A40	51.31	Licorisoflavan A	437 > 391	+	–
A19	36.78	Licorice saponin G2	837 > 351	+	+	A41	51.76	Licorisoflavan B	423 > 335	+	–
A20	37.53	Licorice saponin G2 isomer	837 > 351	+	+	A42	52.21	3-Hydroxyglabrol I	407 > 351	+	–
A21	38.05	Naringenin	271 > 151	+	+	A43	52.32	Gancaonin E	423 > 367	+	–
A22	38.81	Licorice saponin G2 isomer	837 > 351	+	+	A44	52.49	Glyasperin A	421 > 365	+	–

[a] Detected.
[b] Not detected.

Table 2
Metabolites of SNS in rat plasma and urine after oral administration of a high dosage (H) and normal dosage (N) of SNS.

No.	t_R (min)	$[M-H]^-$	Major fragments	λ_{max} (nm)	Log P[a]	Identification	MRM transition	Plasma	Urine
M1	9.91	301	175, 125			Pyrogallol-1-O-glucuronide	301 > 125	–[b]	H, N
M2	11.71	263	183, 168, 124		−0.578	3-O-methylgallic acid-4-O-sulfate	263 > 183	–	H, N
M3	12.49	263	183, 168, 124		−0.828	4-O-methylgallic acid-3-O-sulfate	263 > 183	–	H
M4	12.60	315	175, 125	250		2-O-methylpyrogallol-1-O-glucuronide	315 > 125	–	H, N
M5	14.73	205	125		−1.115	Pyrogallol-1-O-sulfate	205 > 125	–	H, N
M6	15.20	205	125		−1.185	Pyrogallol-2-O-sulfate	205 > 125	–	H
M7	15.51	189	109	270		2-deoxy-pyrogallol-1-O-sulfate	189 > 109	–	H, N
M8	15.69	183	168, 124	215, 255		4-O-methylgallic acid	183 > 168	–	H, N
M9	18.05	273	193			Sulfate conjugate	273 > 193	–	H, N
M10	18.18	203	123			Sulfate conjugate	203 > 123	–	H
M11	18.25	336	160	255, 330		Glucuronide conjugate	336 > 160	–	H, N
M12	18.83	347	267			Sulfate conjugate	347 > 267	–	H
M13	19.78	242	162			Sulfate conjugate	242 > 162	–	H
M14	19.82	511	431, 335		−1.285	Liquiritigenin-4′-O-glucuronide-7-O-sulfate	511 > 431		H
M15	20.87	511	431, 335		−1.285	Liquiritigenin-7-O-glucuronide-4′-O-sulfate	511 > 431	–	H
M16	20.98	257	177, 135, 107			5,7-Dihydroxychromone-O-sulfate	257 > 177	–	H, N
M17	21.46	527	351, 447			Naringenin-O-glucuronide-O-sulfate	527 > 351	–	H, N
M18	23.65	283	107			Glucuronide conjugate	283 > 107	–	H, N
M19	24.09	431	255, 175, 135, 119	270	0.366	Liquiritigenin-4′-O-glucuronide	431 > 255	H	H
M20	24.68	431	255, 175, 135, 119	275	0.082	Liquiritigenin-7-O-glucuronide	431 > 255	H, N	H, N
M21	25.05	333	253			7,4′-Dihydroxyflavone-O-sulfate	333 > 253	–	H, N
M22	25.99	281	201			Sulfate conjugate	281 > 201	–	H
M23	26.79	335	255, 135, 119		0.974	Liquiritigenin-4′-O-sulfate	335 > 255	–	H
M24	27.29	447	271, 175, 151, 119	283	0.470	Naringenin-4′-O-glucuronide	447 > 271	H, N	H, N
M25	27.71	447	271, 175, 151, 119	284	0.406	Naringenin-7-O-glucuronide	447 > 271	H, N	H, N
M26	27.82	389	309			Sulfate conjugate	389 > 309	–	H
M27	28.19	477	301, 175	286	0.256	Hesperetin-7-O-glucuronide	477 > 301	H, N	H, N
M28	28.20	177	135, 91			5,7-Dihydroxychromone	177 > 135	–	H, N
M29	28.30	335	255, 135, 119		0.690	Liquiritigenin-7-O-sulfate	335 > 255	H	H
M30	29.13	477	301, 175	286	0.209	Hesperetin-3′-O-glucuronide	477 > 301	H	H
M31	30.26	514				Unidentified		H, N	–
M32	30.47	351	271, 151, 119			Naringenin-O-sulfate	351 > 271	H, N	H, N
M33	30.60	431	255, 175, 135, 119	369		Isoliquiritigenin-O-glucuronide	431 > 255	H, N	H, N
M34	30.62	533	357, 277, 197			Dimethylgallic acid-O-glucuronide-di-O-sulfate	533 > 357	–	H, N
M35	30.71	514				Unidentified		H, N	–
M36	31.15	512				Unidentified		H, N	–
M37	31.23	514				Unidentified		H, N	–
M38	31.67	514				Unidentified		H, N	–
M39	32.12	512				Unidentified		H, N	–
M40	32.41	514				Unidentified		H, N	–
M41	32.85	512				Unidentified		H, N	–
M42	33.29	498				Unidentified		H, N	–
M43	33.37	255	135, 119	275		Liquiritigenin	255 > 135	H, N	H, N
M44	33.72	381	301, 151		0.974	Hesperetin-3′-O-sulfate	381 > 301	H	H, N
M45	33.95	512				Unidentified		H, N	–
M46	34.02	510				Unidentified		H, N	–
M47	34.10	335	255, 119	372		Isoliquiritigenin-O-sulfate	335 > 255	H	H, N
M48	34.40	567	389, 213, 175			Glucuronide conjugate	389 > 213	–	H, N
M49	35.69	347	267			Fomononetin-O-sulfate	347 > 267	–	H, N
M50	35.82	498				Unidentified		H, N	–
M51	36.69	514				Unidentified		H, N	–
M52	36.74	293	213			Sulfate conjugate	293 > 213	H	–
M53	36.80	381	301, 151		0.690	Hesperetin-7-O-sulfate	381 > 301	H	H, N
M54	37.78	498				Unidentified		H, N	–
M55	38.05	271	227, 151	286		Naringenin	271 > 151	H, N	H, N
M56	39.36	301	257, 151	286		Hesperetin	301 > 151	H, N	H, N
M57	40.04	498				Unidentified		H, N	–
M58	40.38	498				Unidentified		H, N	–
M59	40.69	255	135, 119	372		Isoliquiritigenin	255 > 135	H, N	H, N
M60	42.07	267	252, 223			Fomononetin	267 > 252	H	H, N
M61	47.91	251	207			Unidentified	251 > 107	–	H
M62	53.66	645	469			Glycyrrhetinic acid-O-glucuronide	645 > 469	H, N	H, N
M63	54.31	645	469			Glycyrrhetinic acid-O-glucuronide	645 > 469	H	H, N
M64	56.52	485	441, 425			Hydroxyglycyrrhetinic acid	485 > 441	H, N	H, N
M65	57.58	469	425			Glycyrrhetinic acid[a]	469 > 425	H, N	H

[a] Predicted with chembiodraw ultra 11.0 software.
[b] Not detected.

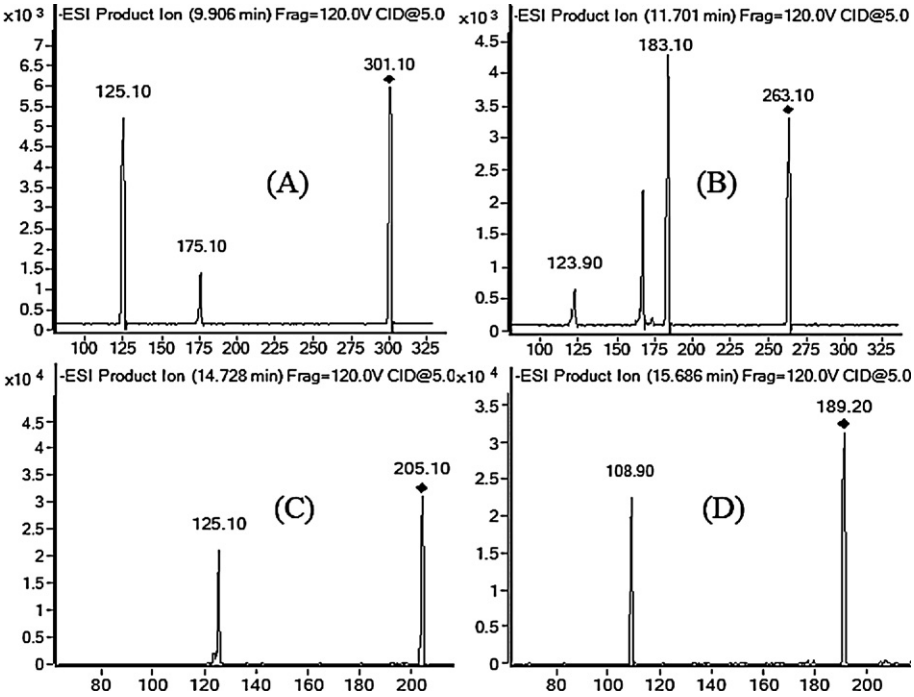

Fig. 4. MS/MS spectra of gallic acid-related metabolites: (A) M1, (B) M2, (C) M5 and (D) M7.

and M3 (12.49 min, log P = −0.828) were preferably assigned to be 4-O-methylgallic acid-3-O-sulfate and 3-O-methylgallic acid-4-O-sulfate, respectively. M4 gave a $[M-H]^-$ molecule at m/z 315, which is the mass of a methyl group (15 Da) more than M1. Characteristic fragment ion at m/z 125 produced from pyrogallol residue was also observed. M4 thus was characterized as 2-O-methylpyrogallol-1-O-glucuronide. M5, M6 and M7 showed main fragment ion at m/z 125 and 109 respectively by a neutral loss of 80 Da, indicating they were sulfation metabolites (Fig. 4C and D). M8 gave a deprotonated molecular ion at m/z 183 and further produced a $[M-H-CH_3]^-$ ion at m/z 168 and a $[M-H-CH_3-COO]^-$ ion at m/z 124, corresponding to the galloyl radical and a 3,4,5-trihydroxybenzoyl group. By referring to literature [28,29], Therefore, M8 was tentatively identified as 4-O-methylgallic acid. The λ_{max} 270 nm (lower) in the DAD spectra of M7 was consistent with that of gallic acid, whereas M8 displayed a λ_{max} 255 nm. Meanwhile, the λ_{max} 215 nm of M8 was consistent with that of gallic acid, whereas M7 did not show a λ_{max} 215 nm (Fig. 5). These findings suggested sulfation of gallic acid lead to no changes in λ_{max} value, while methylation resulted in λ_{max} 270 nm hypsochromic shifts of 15 nm and decarboxylation resulted in the disappearance of λ_{max} 215 nm. M34 gave a $[M-H]^-$ molecule at m/z 533. A CID product ion spectrum of M59 displayed fragment ions at m/z 357 $[M-H-176]^-$, 277 $[M-H-176-80]^-$, and 197 $[M-H-176-2\times80]^-$, which strongly suggest the presence of a glucuronic acid and two sulfuric acid attached to the dimethylgallic acid skeleton. Thus M34 was characterized as dimethylgallic acid-O-glucuronide-di-O-sulfate.

3.4.2. Identification of flavanones-related metabolites

Considering the complicated flavanones such as liquiritin, naringin, hesperidin, and neohespridin in SNS, we firstly studied the metabolism of liquiritin standard individually and ten metabolites were found. A proposed metabolic pathway of liquiritin in rats was shown in Fig. 6. Liquiritin was first metabolized by β-D-glucosidases *in vivo* and converted into its aglycone liquiritigenin (M43). Previously, liquiritigenin has been found to form five kinds of conjugates (4′-O-glucuronide (m1), 7-O-glucuronide (m2), 4′,7-O-disulfate (m3), 4′-O-glucuronide-7-O-sulfate (m4) and 7-O-glucuronide-4′-O-sulfate (m5)) [30]. In this research, M19, M20 and M33 were detected as major metabolites of liquiritin and showed the $[M-H]^-$ ion at m/z 431which further lose a glucuronic acid moiety (176 Da) to produce the aglycone ion at m/z 255. Furthermore, fragments at m/z 135 and119 suggested that there should be one hydroxyl substitution on each of the A and B rings, which was in agreement with the RDA fragmentation for liquiritin [31]. Isomerization into chalcones was also common for liquiritin. Metabolite 33 and 59 showed an absorption maximum typical for chalcones at 369 nm, and were characterized as isoliquiritigenin-O-glucuronide and isoliquiritigenin, respectively. M19 (24.09 min) and M20 (24.68 min) showed an absorption maximum typical for flavanones at 270 nm and 278 nm respectively and were characterized as liquiritigenin-4′-O-glucuronide (log P = 0.366) and liquiritigenin-7-O-glucuronide (log P = 0.082) correspondingly. Based on the characteristic neutral loss of 80 Da and log P values, M19 and M20 were proposed as liquiritigenin-4′-O-sulfation and liquiritigenin-7-O-sulfation, respectively. Meanwhile, 4′-O-glucuronide-7-O-sulfation (M14) and 7-O-glucuronide-4′-O-sulfation (M15) was also found.

Other flavanone glycosides such as isonaringin, naringin, hesperidin, and neohesperidin could also be converted into their aglycones by hydrolysis. Phase II reactions including glucuronidation and sulfation were the major metabolites and their structures were identified similarly. These data were consistent with the reports on biotransformation pathway of naringin and hesperidin [32–35]. Furthermore, hesperetin-7-O-glucuronide (M27) and hesperetin-3′-O-glucuronide (M30) have been confirmed by authentic compounds [32–34]. Their retention times consist with our findings, suggesting that our present method based on log P value is effective and reliable.

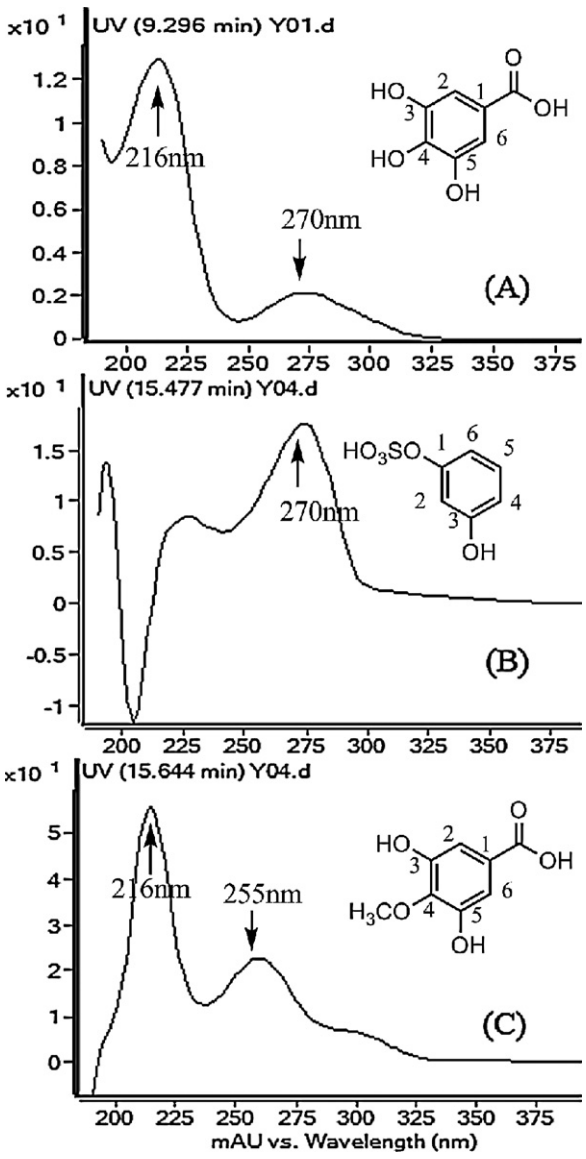

Fig. 5. DAD spectra of gallic acid-related metabolites: (A) gallic acid, (B) M7 and (C) M8.

3.4.3. Identification of glycyrrhizic acid-related metabolites

Glycyrrhizic acid, a representative triterpenoid saponin in SNS, was detected in high abundance in plasma after orally administered to rats. Glycyrrhizic acid was readily to lose one or two molecules of glucuronic acid to produce glycyrrhetinic acid-O-glucuronide (M63) and glycyrrhetinic acid (M65), respectively, indicating that hydrolysis was the major metabolic fate of glycyrrhizic acid. This is in consistent with literature [36]. In addition, a hydroxylated derivative of glycyrrhetinic acid (M64) was also observed in plasma. It might be hydroxylated at C-22α or C-24, according to the previous report on glycyrrhetinic acid metabolism [37].

In contrast to those phenolic aglycones which were usually metabolized to conjugated metabolites, no conjugated metabolism was found for glycyrrhizic acid, suggesting that the activities of phase II metabolic enzymes toward phenols were significantly higher than alcohols [38]. Although many triterpenoid saponins such as licorice saponin A3, B2 and G2 were detected in rat plasma after oral administration of SNS extract, glycyrrhizic acid and glycyrrhetinic acid were the predominant metabolites, suggesting saponin aglycones were the major circulating forms of glycyrrhizic acid-related compounds.

3.4.4. Identification of other metabolites

Paeoniflorin is one of the main monoterpene glycosides in Radix *Paeoniae Alba*.

Previous studies had reported low bioavailability of orally administered paeoniflorin in rats (approximately 3–4%) [39,40], Metabolism of paeoniflorin is an important mechanism that is responsible for poor bioavailability of paeoniflorin. Administered paeoniflorin was extensively metabolized into paeoniflorgenin, paeonimetabolins I and II [41–43]. However, none of the three metabolites were detected in the present study. An earlier study indicated that higher plasma concentrations of paeoniflorin were achieved by using a more crude extract of the plant [44]. Additional reports showed that higher plasma concentrations of paeoniflorin were achieved when it is included as a part of multiple herb formula: Shao-yao Gan-chao Tang [45]. These results indicated that the bioavailability of paeoniflorin could be improved by other phytochemicals present in the herbal formula. Similarly we did not found the formation of saikogenin F [46], an aglycone (metabolite) of saikosaponin a. These results suggested that the other chemical components may influence the metabolites of single compound.

It should be mentioned that although we detected a lot metabolites, the structures of some metabolites were not established due to no or limited structural information.

Among them a group of metabolites with $[M-H]^-$ ions at m/z 498–514 attached our interest. These metabolites gave no fragmentation under CID or a high 375 V fragmentor. Since the obvious limitation of LC–MS in the structural elucidation of these metabolites has shown, other technology such as LC-NRM is required for further study.

3.5. Analysis of normal dosage bio-samples by MRM

Although a high dosage increases the plasmatic concentrations of the components of SNS and their metabolites, these values are no longer related to the therapeutic concentrations. Thus it is very important to profile SNS metabolites at an oral clinical dosage. At such a low dose, most metabolites could not be detected by examining total ion current chromatograms (TICs). Therefore, in this step of our strategy, we used a highly sensitive and selective multiple reaction monitoring (MRM) technique to detect the metabolites since tandem mass spectrometry using MRM has a lower limit of detection than scanning mass spectrometry [47]. However, MRM is a targeted rather than a discovery-based global expedition. To use MRM, one needs to know the structures of possible metabolites. Fortunately, this information had already been obtained from the high dosage bio-samples which could be used as a metabolite data-base for normal dosage bio-samples. The structures of metabolites characterized in the high dosage bio-samples, as well as their MS/MS spectral data were used to set the ion pairs for MRM detection. By using the MRM method, most of the pre-characterized metabolites gave an obvious signal even though the matrix was very complicated and the concentrations were fairly low (Fig. 7). However, some metabolites discovered in high dosage bio-samples were not detected in the normal ones. Given the good sensitivity of MRM technique, it was unlikely these compounds could not be detected. Instead, we consider that single compound dosing or too high dosage may change the absorption of rat intestine. Finally, 36 absorbed compounds and 29 metabolites in plasma and 33 metabolites in urine were detected after oral administration of SNS at a normal dosage of 1 g/kg (Table 2).

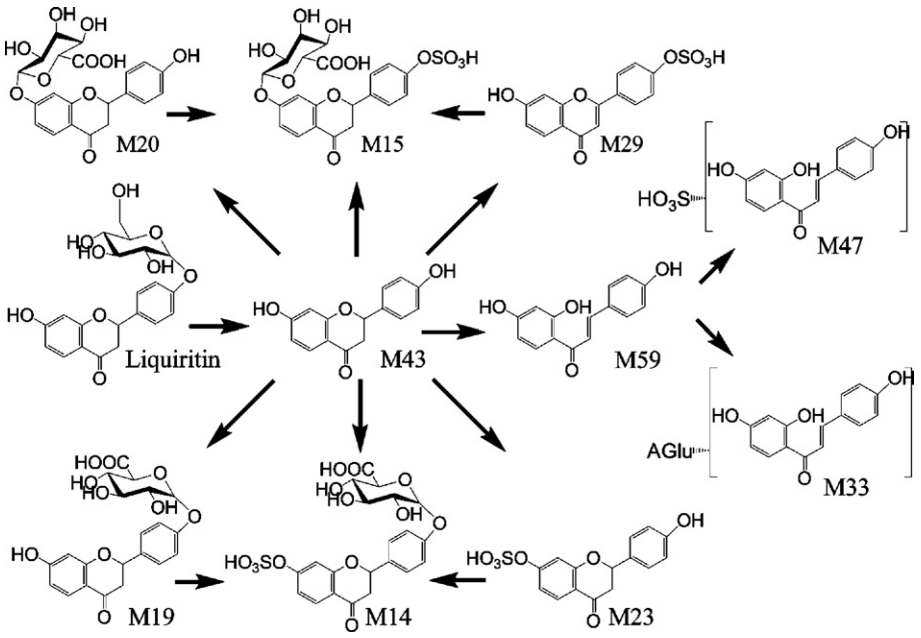

Fig. 6. A proposed metabolic pathway of liquiritin in rats.

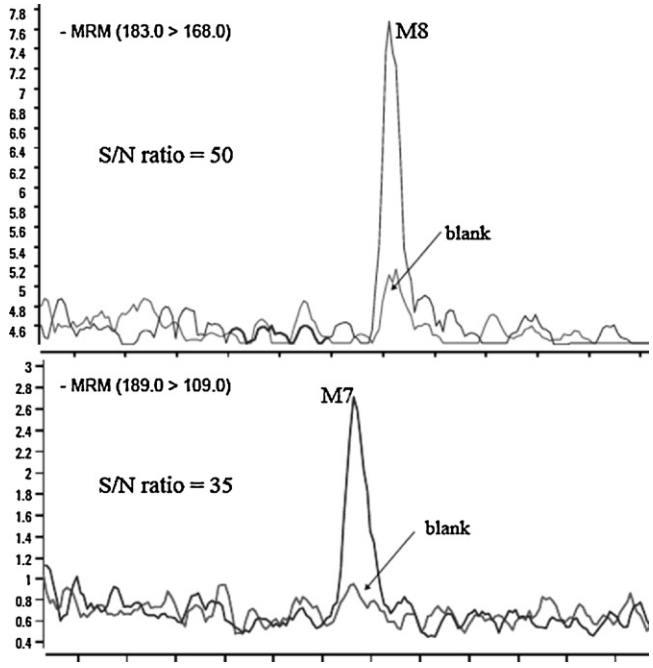

Fig. 7. Overlay of MRM chromatograms of M7 and M8 in normal dose urine sample with a blank.

4. Conclusions

In summary, we have developed a LC-DAD–MS/MS based approach and proposed a useful strategy to systematically characterize the *in vivo* metabolites of a traditional Chinese medicine formula (TCMF), SNS. After an oral administration of SNS extract at a normal clinical dosage, 36 absorbed compounds and 29 metabolites in plasma and 33 metabolites in urine were detected by a highly sensitive MRM method. Although the metabolism and the metabolites of the saikosaponin and paeoniflorin have been reported in the literature, no metabolites of saikosaponin and paeoniflorin were detected in the present study. These results suggested that the other chemical components may influence the metabolites of single compound. Meanwhile, a new metabolite of glycyrrhizic acid (glycyrrhetinic acid-O-glucuronide) was also found. This investigation would effectively narrow the range of potentially bioactive constituents of SNS and shed light to its action mechanism. Moreover, the developed strategy and approach may also be extended to investigate the metabolism of other TCMF.

Acknowledgments

This work was financially supported by the Priority Academic Program Development of Jiangsu Higher Education Institutions, China (Grant no. 201101096), Jiangsu research program for industrialization of research findings of the Higher Education Institutions, China (Grant no. JH10-21).

Appendix A. Supplementary data

Supplementary data associated with this article can be found, in the online version, at doi:10.1016/j.jchromb.2011.12.017.

References

[1] X.P. Guo, D.L. Li, J.M. Li, Z.G. Liu, Y.M. Wang, Chin. J. Inform. Trad. Chin. Med. 22 (1999) 71.
[2] F.W. Zhang, Y. Zhang, Chin. J. Trad. Chin. Med. Pharm. 15 (2000) 79.
[3] S.R. Cai, H.T. Liu, J. Sichuan Trad. Chin. Med. 22 (2004) 47.
[4] J. Jiang, C. Zhou, Q. Xu, Biol. Pharm. Bull. 26 (2003) 1089.
[5] Y. Sun, T. Chen, Q. Xu, J. Pharm. Pharmacol. 55 (2003) 839.
[6] L. Zhang, Y. Dong, Y. Sun, T. Chen, Q. Xu, J. Pharm. Pharmacol. 58 (2006) 1257.
[7] Y. Sun, T.T. Cai, Y. Shen, X.B. Zhou, T. Chen, Q. Xu, Int. Immunopharmacol. 9 (2009) 1437.
[8] L. Zhang, Y. Sun, T. Chen, Q. Xu, Int. Immunopharmacol. 5 (2005) 1193.
[9] Y. Sun, Y. Dong, H.J. Jiang, T.T. Cai, L. Chen, X. Zhou, T. Chen, Q. Xu, Life Sci. 84 (2009) 334.
[10] H. Liu, X.H. Yang, P. Zi, F. Liu, H.F. Kuang, J. Nanjing Norm. Univ. 30 (2007) 75.
[11] H.J. Sim, J.S. Jeong, H.J. Kwon, Y.M. Lee, S.P. Hong, J. Chromatogr. A 1217 (2010) 5302.
[12] Z.X. Yan, C. Chen, Y. Chen, X.B. Xie, B. Fu, J. Zhang, J.B. Wu, X.H. Yang, Analyst, under review.
[13] G. Ye, Y.H. Tang, G.Y. Wang, Z.X. Li, H.Y. Zhu, C.H. Ma, Z.L. Sun, C.G. Huang, Chem. Biodivers. 7 (2010) 2917.
[14] R. Song, L. Xu, F.G. Xu, Z. Li, H.J. Dong, Y. Tian, Z.J. Zhang, J. Chromatogr. A 1217 (2010) 7144.

[15] A. Zuniga, L. Li, Anal. Chim. Acta 689 (2011) 77.
[16] S.L. Su, J.M. Guo, J.A. Duan, T.J. Wang, D.W. Qian, E.X. Shang, Y.P. Tang, J. Chromatogr. B 878 (2010) 355.
[17] S.M. Ni, D.W. Qian, J.A. Duan, J.M. Guo, E.X. Shang, Y. Shu, C.F. Xue, J. Chromatogr. B 878 (2010) 2741.
[18] C.S. Wu, Y.X. Sheng, Y.H. Zhang, J.L. Zhang, B.L. Guo, Rapid Commun. Mass Spectrom. 22 (2008) 2813.
[19] A. Kamleh, M.P. Barrett, D. Wildridge, R.J. Burchmore, R.A. Scheltema, D.G. Watson, Rapid Commun. Mass Spectrom. 22 (2008) 1912.
[20] W.J. Lambert, J. Chromatogr. A 656 (1993) 469.
[21] D.J. Minick, D.A. Brent, J. Frenz, J. Chromatogr. 461 (1989) 177.
[22] W. Zhang, M.W. Saif, G.E. Dutschman, X. Li, W. Lam, S. Bussom, Z.L. Jiang, M. Ye, E. Chu, Y.C. Cheng, J. Chromatogr. A 1217 (2010) 5785.
[23] W. Mullen, A. Boitier, A.J. Stewart, A. Crozie, J. Chromatogr. A 1058 (2004) 163.
[24] O.A. Heikal, T. Akao, S. Takeda, M. Hattori, Biol. Pharm. Bull. 20 (1997) 517.
[25] V. Crepy, C. Morand, J. Agric. Food Chem. 50 (2002) 618.
[26] J.O. Miners, P.A. Smith, M.J. Sorich, R.A. McKinnon, P.I. Mackenzie, Annu. Rev. Pharmacol. Toxicol. 44 (2004) 1.
[27] L. Zong, M. Inoue, M. Nose, K. Kojima, N. Sakaguchi, K. Isuzugawa, T. Takeda, Y. Ogihara, Biol. Pharm. Bull. 22 (1999) 326.
[28] T. Yasuda, A. Inaba, M. Ohmori, T. Endo, S. Kubo, K. Ohsawa, J. Nat. Prod. 63 (2000) 1444.
[29] S. Shahrzad, I. Bitsh, J. Chromatogr. B 705 (1998) 87.
[30] H. Shimamura, H. Suzuki, M. Hanano, A. Suzuki, Y. Sugiyama, Biol. Pharm. Bull. 16 (1993) 899.
[31] G.G. Tan, Z.Y. Zhu, H. Zhang, L. Zhao, Y. Liu, X. Dong, Z.Y. Lou, Rapid Commun. Mass Spectrom. 24 (2010) 209.
[32] H. Matsumoto, Y. Ikoma, M. Sugiura, M. Yano, Y. Hasegawa, J. Agric. Food Chem. 52 (2004) 6653.
[33] A. Trzeciakiewicz, V. Habauzit, S. Mercier, J. Agric. Food Chem. 58 (2010) 668.
[34] L. Bredsdorff, I.L.F. Nielsen, S.E. Rasmussen, C. Cornett, D. Barron, F. Bouisset, E. Offord, G. Williamson, Br. J. Nutr. 103 (2010) 1602.
[35] T.Z. Fang, Y.G. Wang, Y. Ma, W.W. Su, Y. Bai, P.Y. Zhao, J. Pharm. Biomed. Anal. 40 (2006) 454.
[36] Z.P.J. Lin, S.X. Qiu, A. Wufuer, L. Shum, J. Chromatogr. B 814 (2005) 201.
[37] K. Gao, Y. Wei, J. Yang, X.H. Duan, Chin. Clin. Pharmacol. Ther. 12 (2007) 1255.
[38] P.D.L. Chao, S.L. Hsiu, Y.C. Hou, J. Food Drug Anal. 11 (2002) 35.
[39] S. Takeda, T. Isono, Y. Wakui, Y. Matsuzaki, H. Sasaki, S. Amagaya, J. Pharm. Pharmacol. 47 (1995) 1036.
[40] S. Takeda, T. Isono, Y. Wakui, Y. Mizuhara, S. Amagaya, M. Maruno, M. Hattori, J. Pharm. Pharmacol. 49 (1997) 35.
[41] C.H. Wang, R. Wang, X.M. Cheng, Y.Q. He, Z.T. Wang, C. Wu, J. Cao, J. Ethnopharmacol. 117 (2008) 467.
[42] S.L. Hsiu, Y.T. Lin, K.C. Wen, P.D. Chao, Planta Med. 69 (2003) 1113.
[43] M. Hattori, Y.Z. Shu, M. Shimizu, T. Hayashi, N. Morita, X.G. Kobashi, T. Namba, Chem. Pharm. Bull. 33 (1985) 3838.
[44] L.C. Chen, M.H. Lee, M.H. Chou, M.F. Lin, L.L. Yang, J. Chromatogr. B 735 (1999) 33.
[45] L.C. Chen, M.H. Chou, M.F. Lin, L.L. Yang, Jpn. J. Pharmacol. 88 (2002) 250.
[46] K. Shimizu, S. Amagaya, Y. Ogihara, J. Pharmacobiodyn. 8 (1985) 718.
[47] I.S. Lurie, S.G. Toske, J. Chromatogr. A 1188 (2008) 322.